

# Uncertainty Bounds for Gramian-Based Interaction Measures

BJÖRN HALVARSSON

Uppsala University  
Dept. of Information Technology  
P O Box 337, SE-751 05 Uppsala  
SWEDEN

Bjorn.Halvarsson@it.uu.se

MIGUEL CASTAÑO

Luleå University of Technology  
Dept. of Comp. Sci. and Elect. Eng.  
SE-971 87 Luleå  
SWEDEN

miguel.castano@ltu.se

WOLFGANG BIRK

Luleå University of Technology  
Dept. of Comp. Sci. and Elect. Eng.  
SE-971 87 Luleå  
SWEDEN

wolfgang.birk@ltu.se

*Abstract:* Bounds of two Gramian-based Interaction Measures (IM:s) induced by model uncertainty are presented in this paper. The connection between the considered IM:s (the Hankel Interaction Index Array (HIIA) and the Participation Matrix (PM)) is explored, showing that it is possible in certain cases to translate the bounds of one into bounds of the other. The first method is a tightening of previously suggested uncertainty bounds for the HIIA. The second method is based on a novel exploration of the relationship between the PM and the area enclosed by the Nyquist diagram. The latter method is a numerical approximation of the analytical bounds of the PM, whilst the former one provides very loose bounds for the examples presented here .

*Key-Words:* interaction measures, multivariable systems, input-output pairing, control structure selection, system gramians, model uncertainties

## 1 Introduction

Interaction measures (IM:s) aim at quantifying the impact of loop interaction in multivariable systems and are of practical use to decide on appropriate control structures for a process.

Already in the 1960:s the Relative Gain Array (RGA) was proposed by Bristol [2], and it is still the most commonly used IM. Later, Gramian-based IM:s like the Hankel Interaction Index Array (HIIA) and the Participation Matrix (PM) were suggested (see [13, 4, 11]) as an alternative to the RGA, in order to overcome its shortcomings. Despite the fact that process models are usually affected by modeling uncertainties, IM:s are solely applied to nominal models, raising the question of their validity. Recently, researchers have started to address this problem.

A process model with model uncertainties can be understood as a set of process models which includes the nominal model. Therefore, the value of the IMs may differ for different models in the set. Including model uncertainties in the interaction analysis would enable robust decisions in the control structure selection. In [9], an inequality expressing the maximum variation of the HIIA in the presence of additive uncertainties in the state space matrices of a process model was derived.

In this paper, based on the results of [9] a tighter uncertainty bound is proposed in Section 3.2. It is also shown how this bound relates to an uncertainty bound for the PM. Furthermore, a novel method to obtain analytical bounds for the PM is derived in Section 3.3,

which yields even tighter uncertainty bounds for both the HIIA and the PM. Finally, the methods are compared in two illustrative examples, and the usefulness of the bounds is discussed.

## 2 Gramian-based IM:s

The controllability and observability Gramians,  $P$  and  $Q$ , are obtained by solving the following two continuous-time Lyapunov equations [12]:

$$AP + PA^T + BB^T = 0, \quad A^T Q + QA + C^T C = 0,$$

where  $A$ ,  $B$  and  $C$  are the system matrices in the corresponding state-space description  $(A, B, C, 0)$ . The product  $PQ$  collects important information about the controllability and observability of the system. Besides, it can be shown that the Hankel singular values (HSV:s) are equal to the positive square root of the eigenvalues of  $PQ$  and they have important implications in quantifying the process dynamics.

This forms the base of the Hankel Interaction Index Array (HIIA) and the Participation Matrix (PM): two Gramian-based IM:s which consider that the most important input-output channels are those with larger values of the HSV:s.

The HIIA was introduced in [13]. It considers only the largest HSV of each input-output system, and it can be expressed as a function of the HSV:s or the largest eigenvalue of  $PQ$ :

$$[\Sigma_H]_{ij} = \frac{\|G_{ij}\|_H}{\sum_{kl} \|G_{kl}\|_H} = \frac{\sqrt{\lambda_{\max}(P_j Q_i)}}{\sum_{kl} \sqrt{\lambda_{\max}(P_l Q_k)}}$$

where  $\|G_{ij}\|_H$  denotes the Hankel norm of  $G_{ij}$ , which is the largest HSV of the subsystem with input  $u_j$  and output  $y_i$  of the stable system  $G$ .

PM was introduced in [4]. It considers all the HSV:s of each input-output system and can be expressed as a function of the HSV:s or the eigenvalues of  $PQ$ .

$$\phi_{ij} = \frac{\|G_{ij}\|_{HS}^2}{\sum_{kl} \|G_{kl}\|_{HS}^2} = \frac{tr(P_j Q_i)}{\sum_{kl} tr(P_l Q_k)}$$

where  $\|G_{ij}\|_{HS}$  denotes the Hilbert-Schmidt (HS) norm of  $G_{ij}$ , which is defined as the square root of the sum of the squared HSV:s of the subsystem  $G_{ij}$ . Moreover,

$$\|G_{ij}\|_{HS}^2 = tr(P_j Q_i). \quad (1)$$

A matrix collecting the value of the Hankel norm of each SISO subsystem will be called unnormed HIIA and denoted  $\tilde{\Sigma}_H$ . When the HS norm is considered, it will be called unnormed PM and denoted  $\tilde{\Phi}$ . The aim is to find the a control structure of low complexity that gives a large sum of the contributions.

The cross-Gramian matrix  $W_{co}$  was introduced in [9], and it is obtained by solving the Sylvester equation

$$W_{co}A + AW_{co} = -BC.$$

Using the cross-Gramian, the Hankel and HS norms can be computed as [9]

$$\|G_{ij}(s)\|_H = \sqrt{\lambda_{max}((W_{co}^{ij})^2)} = max|\lambda(W_{co}^{ij})|,$$

$$\|G_{ij}\|_{HS}^2 = tr((W_{co}^{ij})^2).$$

This way, only one linear matrix equation needs to be solved to obtain the Hankel norm and the HIIA, which simplifies the derivation of uncertainty bounds suggested for the HIIA.

### 3 Results on the uncertainty analysis

#### 3.1 Relating the HIIA with the PM

The Hankel norm can be obtained from the unnormed PM, and vice versa, by comparing the HSV:s:

$$\|G_{ij}\|_H = \eta_{ij} \sqrt{tr(P_j Q_i)} \quad (3)$$

where  $\eta_{ij}$  is the square root of the quotient between the maximum HSV and the sum of the HSV:s

$$\eta_{ij} = \sqrt{\frac{\lambda_{max}(P_j Q_i)}{\sum_k \lambda_k(P_j Q_i)}} \leq 1. \quad (4)$$

We will use this quotient to obtain the bounds of the unnormed HIIA due to uncertainty from previously computed bounds for the unnormed PM. Note that this

quotient may be affected by the introduction of uncertainties in the model. However, some special cases have been identified:

- First order models will always have  $\eta = 1$  (there is only one HSV in this case).
- $\eta$  is insensitive to uncertain gains affecting the system since they will appear as common factors in both the numerator and the denominator of  $\eta$ .
- Elements in the quotient with a value close to 1 are expected to be robust to uncertainties. The HSV:s of many systems decay extremely rapidly [1]. Thus, a reduced order model can be created by truncating the states which are related to the smaller HSV:s [1]. Elements in  $\eta$  which are close to 1 indicate the existence of a highly dominating HSV, and the uncertainty affecting the smaller HSV:s can therefore be disregarded since it will introduce neglectable variations in the quotient.

#### 3.2 Uncertainty bounds for HIIA and PM

Consider the following continuous-time system with additive uncertainty

$$\begin{aligned} \dot{x}(t) &= (A + \Delta A)x(t) + (B + \Delta B)u(t), \\ y(t) &= (C + \Delta C)x(t). \end{aligned} \quad (5)$$

Assume that the upper bounds of  $\|\Delta A\|$ ,  $\|\Delta b_{*j}\|$  and  $\|\Delta c_{i*}\|$  are known where  $\Delta b_{*j}$  is the additive uncertainty in the  $j$ :th column of  $B$ ,  $\Delta c_{i*}$  is the additive uncertainty in the  $i$ :th row of  $C$  and  $\|\cdot\|$  denotes the 2-norm. First note that  $\|\Delta W_{co}^{ij}\|$  is an upper bound of the additive uncertainty in the Hankel norm  $\|G_{ij}\|_H$  since

$$\begin{aligned} \|G_{ij}\|_H &= \sqrt{\lambda_{max}((W_{co}^{ij})^2)} \\ &\leq \sqrt{\lambda_{max}((W_{co}^{ij})^H (W_{co}^{ij}))} = \|W_{co}^{ij}\|. \end{aligned}$$

An upper bound of the additive uncertainty of  $W_{co}^{ij}$  is derived by Moaveni and Khaki-Sedigh [9] and is given, in terms of the 2-norm by

$$\begin{aligned} \Delta \|G_{ij}\|_H &\leq \|\Delta W_{co}^{ij}\| \leq \|\Delta W_{co}^{ij}\|_F \leq \\ &\left\| (I_n \otimes A + A^T \otimes I_n)^{-1} \cdot \left( 2n \|\Delta A\| \|W_{co}^{ij}\| + \right. \right. \\ &\left. \left. \|b_{*j}\| \|\Delta c_{i*}\| + \|\Delta b_{*j}\| \|c_{i*}\| + \|\Delta b_{*j}\| \|\Delta c_{i*}\| \right) \right\|. \end{aligned} \quad (6)$$

where  $\otimes$  is the Kronecker product,  $b_{*j}$  is the  $j$ :th column of  $B$ ,  $c_{i*}$  is the  $i$ :th row of  $C$  and  $\|\cdot\|_F$  denotes the Frobenius norm.

The aim of this section is to propose a new bound on  $\|\Delta W_{co}^{ij}\|_F$  which is tighter than the bound in (6) when  $\Delta A$  and/or  $W_{co}^{ij}$  have not full rank. It is also shown that it is a bound for the additive uncertainty

on the square root of the unnormed PM. As a final result, the latter bound is converted into the bound for the additive uncertainty on the Hankel norm by using the quotient  $\eta$  in (4).

**Theorem 1** Consider the MIMO system with additive uncertainty in (5). An upper bound of the additive parametric uncertainty in  $W_{co}^{ij}$  is then given by

$$\begin{aligned} \|\Delta W_{co}^{ij}\|_F &\leq \left\| (I_n \otimes A + A^T \otimes I_n)^{-1} \right\| \\ &\cdot \left( 2\sqrt{r_{\Delta A} r_{W_{co}^{ij}}} \|\Delta A\| \|W_{co}^{ij}\| + \|b_{*j}\| \|\Delta c_{i*}\| \right. \\ &\left. + \|\Delta b_{*j}\| \|c_{i*}\| + \|\Delta b_{*j}\| \|\Delta c_{i*}\| \right), \end{aligned} \quad (7)$$

where  $r_{\Delta A}$  is the rank of  $\Delta A$ ,  $r_{W_{co}^{ij}}$  is the rank of  $W_{co}^{ij}$  and  $\eta_{ij}$  is defined in (4).

**Proof:** The bound given in (6) is made tighter using the following inequalities [10]:

$$\|\mathcal{A}\| \leq \|\mathcal{A}\|_F \leq \sqrt{r}\|\mathcal{A}\| \leq \sqrt{n}\|\mathcal{A}\|,$$

where  $r$  is the rank of the  $n \times n$  matrix  $\mathcal{A}$ . Using these inequalities, the factor  $n$  in (6) is replaced by the factor  $\sqrt{r_{\Delta A} r_{\Delta W_{co}^{ij}}}$ .  $\square$

**Remark 2** When  $\sqrt{r_{\Delta A} r_{\Delta W_{co}^{ij}}} < n$ , i.e. when  $\Delta A$  and/or  $W_{co}^{ij}$  are not full rank, and  $\|\Delta A\| \neq 0$ , this makes the bound less conservative.

**Remark 3** The rank of  $\Delta A$  depends on the structure of the uncertainty.

From Theorem 1, an upper bound of the unnormed PM,  $\tilde{\Phi}$ , can easily be derived. This is presented in the following lemma:

**Lemma 4** For each SISO subsystem, an upper bound of the additive uncertainty of the square root of the unnormed PM, denoted  $(\Delta\sqrt{\tilde{\Phi}_{ij}})$ , is given by  $\|\Delta W_{co}^{ij}\|_F$  in Theorem 1. The corresponding uncertainty of  $\tilde{\Phi}$  is

$$\Delta\tilde{\Phi}_{ij} = \left(\Delta\sqrt{\tilde{\Phi}_{ij}}\right)^2 + 2\sqrt{\tilde{\Phi}_{ij}}\left(\Delta\sqrt{\tilde{\Phi}_{ij}}\right).$$

**Proof:** First note that  $\|\Delta W_{co}^{ij}\|_F$  is an upper bound of the uncertainty of  $\sqrt{\tilde{\Phi}_{ij}}$ . This follows from

$$\sqrt{\tilde{\Phi}_{ij}} = \sqrt{\text{tr}((W_{co}^{ij})^2)} \leq \sqrt{\text{tr}((W_{co}^{ij})^H W_{co}^{ij})} = \|W_{co}^{ij}\|_F.$$

Therefore, (6) and the potentially tighter bound (7), are also upper bounds for the uncertainty  $(\Delta\sqrt{\tilde{\Phi}_{ij}})$ .

Finally, we express  $\Delta\tilde{\Phi}_{ij}$  as a function of  $(\Delta\sqrt{\tilde{\Phi}_{ij}})$ :

$$\begin{aligned} \Delta\tilde{\Phi}_{ij} &= \left(\sqrt{\tilde{\Phi}_{ij}} + \left(\Delta\sqrt{\tilde{\Phi}_{ij}}\right)\right)^2 - \tilde{\Phi}_{ij} \\ &= \left(\Delta\sqrt{\tilde{\Phi}_{ij}}\right)^2 + 2\sqrt{\tilde{\Phi}_{ij}}\left(\Delta\sqrt{\tilde{\Phi}_{ij}}\right). \end{aligned}$$

$\square$

**Lemma 5** For each SISO subsystem, an upper bound on the additive uncertainty on the Hankel norm can be calculated from the bound  $\|\Delta W_{co}^{ij}\|_F$  in Theorem 1 by multiplication by the factor  $\eta_{ij}$ ,

**Proof:** It follows from Lemma 4 and the link between the Hankel norm and the unnormed PM in (3).  $\square$

**Remark 6** This is a tighter bound than the one in (6). A first tightening of the bound of  $\|\Delta W_{co}^{ij}\|_F$  was obtained in (7). The bound was further tightened by the factor  $\eta_{ij} \leq 1$ .

### 3.3 Numerical approximation of the PM uncertainty bounds

As shown in [5] the squared HS norm of a SISO stable strictly proper system  $G$  equals  $\pi^{-1}$  times the area enclosed by the oriented Nyquist curve  $(A_c(\Gamma))$ , and therefore from (1):

$$\text{tr}(PQ) = \pi^{-1} A_c(\Gamma(\omega)),$$

where  $\Gamma(\omega) = G(j\omega)$  and  $\omega \in \mathbb{R}$  runs from  $-\infty$  to  $\infty$  in the continuous-time case.

This shows that the PM is in fact closely related to the Direct Nyquist Array (DNA) introduced by Rosenbrock in the early 1970:s (see for instance [8, 6] for an introduction to DNA analysis and [3] for a discussion of DNA in connection with uncertain systems). In the basic DNA approach, Nyquist curves are plotted for each subsystem and the decentralized pairings corresponding to the largest Nyquist curves are selected. Obviously, the PM is a quantitative version of this idea, however, initially derived to quantify controllability and observability of the state space.

The link between the PM and the Nyquist diagram makes it possible to calculate the uncertainty of the unnormed PM by calculating the uncertainty of the area enclosed by the Nyquist diagram of each SISO subsystem. These bounds have the potential of being the analytical bounds, since no inequalities are involved in the calculations.

As an example, independent multiplicative uncertainty in the transfer function of each SISO subsystem is considered. The uncertainty set,  $\Pi$ , is then

$$\Pi_{ij} : G_{P_{ij}}(s) = G_{ij}(s) \cdot (1 + w_{ij}(s) \cdot \Delta_{ij}(s)),$$

where  $G_P(s)$  represents any possible perturbed plant in  $\Pi$ ,  $\Delta_{ij}(s)$  is any stable transfer function with  $|\Delta_{ij}(j\omega)| \leq 1$ . The multiplicative (relative) weight  $w_{ij}(\omega)$  is designed to represent the uncertainty [12].

The uncertainty can be characterized, for each frequency in the Nyquist diagram, as a disc with radius  $|G_{ij}(j\omega)w_{ij}(j\omega)|$  centered at  $G_{ij}(j\omega)$  Fig. 1.

Generally, adding the value of  $|G_{ij}(j\omega)w_{ij}(j\omega)|$  in the direction and sense of the vector normal to the

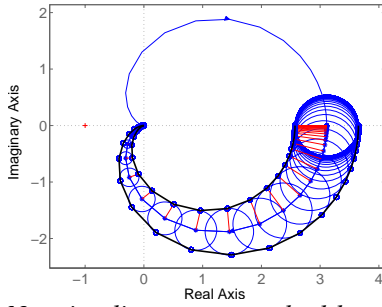


Figure 1: Nyquist diagram perturbed by uncertainty. The nominal Nyquist curve, and the curves enclosing the minimum and maximum areas in the uncertainty set are depicted.

nominal Nyquist curve (see Fig. 1), the curve enclosing the smaller area in the uncertainty set is obtained. Similarly, by adding  $|G_{ij}(j\omega)w_{ij}(j\omega)|$  in the opposite sense, the curve enclosing the larger area in the uncertainty set is obtained. However, this statement may not hold for systems with a large uncertainties and high order. Before proceeding with the integration of the areas, a visual inspection of the validity of these bounds is therefore advised (see Fig. 1).

An analytical description of the boundary curves can be obtained using the Frenet-Serret formulas to calculate the normal vector to the nominal Nyquist curve. Nevertheless, integrating the analytical expression can in many cases be complicated, and numerical area estimation methods can be used instead. In the work presented in this paper, the curves were discretized at a finite number of points, and the function *polyarea* in MATLAB was used to perform the integration.

Additionally, these bounds of the unnormalized PM can be converted into bounds of the unnormalized HIIA using the quotient  $\eta$  described in Section 2.

## 4 Example: the quadruple-tank

The quadruple-tank process was described in [7] and is represented by the following continuous state space model

$$A = \begin{bmatrix} -\frac{1}{T_1} & 0 & \frac{A_3}{A_1 T_3} & 0 \\ 0 & -\frac{1}{T_2} & 0 & \frac{A_4}{A_2 T_4} \\ 0 & 0 & -\frac{1}{T_3} & 0 \\ 0 & 0 & 0 & -\frac{1}{T_4} \end{bmatrix},$$

$$B = \begin{bmatrix} \frac{\gamma_1 k_1}{A_1} & 0 \\ 0 & \frac{\gamma_2 k_2}{A_2} \\ 0 & \frac{(1-\gamma_2)k_2}{A_3} \\ \frac{(1-\gamma_1)k_1}{A_4} & 0 \end{bmatrix}, C = \begin{bmatrix} k_c & 0 & 0 & 0 \\ 0 & k_c & 0 & 0 \end{bmatrix},$$

and with nominal parameter values given in Tab. 1. The time constants are  $T_i = \frac{A_i}{a_i} \sqrt{(2h_i)/g}$ ,

Table 1: Parameter values for the nominal model of the quadruple-tank process.

Parameter:	$A_1, A_3$	$A_2, A_4$	$a_1, a_3$	$a_2, a_4$	$g$	$\gamma_1$	$\gamma_2$
Value:	28	32	0.071	0.057	981	0.42	0.32
Unit:	cm <sup>2</sup>	cm <sup>2</sup>	cm	cm	cm/s <sup>2</sup>	-	-
Parameter:	$h_1$	$h_2$	$h_3$	$h_4$	$k_1$	$k_2$	$k_c$
Value:	13.64	16.55	1.91	1.77	3.33	3.35	0.50
Unit:	cm	cm	cm	cm	$\frac{\text{cm}^3}{\text{Vs}}$	$\frac{\text{cm}^3}{\text{Vs}}$	$\frac{\text{cm}^3}{\text{Vs}}$

$i = 1, \dots, 4$ , and the corresponding transfer function matrix is given by

$$G(s) = \begin{bmatrix} \frac{\gamma_1 c_1}{1 + sT_1} & \frac{(1 - \gamma_2) c_1}{(1 + sT_3)(1 + sT_1)} \\ \frac{(1 - \gamma_1) c_2}{(1 + sT_4)(1 + sT_2)} & \frac{\gamma_2 c_2}{1 + sT_2} \end{bmatrix} \quad (8)$$

where  $c_1 = T_1 k_1 k_c / A_1$  and  $c_2 = T_2 k_2 k_c / A_2$ . An interaction analysis of the nominal plant results in the decentralized pairing suggestion  $y_1-u_2, y_2-u_1$  as seen from the unnormalized HIIA ( $\tilde{\Sigma}_H$ ) and PM ( $\tilde{\Phi}$ ):

$$\tilde{\Sigma}_H = \begin{bmatrix} 0.8212 & 1.5642 \\ 1.8051 & 0.8637 \end{bmatrix}, \tilde{\Phi} = \begin{bmatrix} 0.6744 & 2.4982 \\ 3.3205 & 0.7459 \end{bmatrix}.$$

*Case 1.* Variations on the Hankel norm for this process were analyzed by [9] considering  $\gamma_1$  and  $\gamma_2$  as uncertain parameters. We will consider the same parameter variations  $|\Delta\gamma_1| = 0.1$  and  $|\Delta\gamma_2| = 0.2$ . This implies an uncertainty of  $|\Delta b_{*1}| \leq 0.0158$  and  $|\Delta b_{*2}| \leq 0.0318$  which allow the application of (7) to calculate the bound  $\tilde{\Phi}^{(7)}$ , and a multiplicative uncertainty described by

$$w = \begin{pmatrix} 0.2381 & 0.2941 \\ 0.1724 & 0.6250 \end{pmatrix},$$

which allow the computation of the bounds of  $\tilde{\Phi}$  by integration as described in Section 3.3 to calculate the bound  $\tilde{\Phi}^N$ . The resulting bounds on  $\tilde{\phi}$  are:

$$\tilde{\Phi}^{(7)} \in \begin{bmatrix} [-0.9716, 2.3204] & [-3.9623, 8.9587] \\ [0.2690, 6.3720] & [-3.6893, 5.1810] \end{bmatrix},$$

$$\tilde{\Phi}^N \in \begin{bmatrix} [0.3420, 1.1597] & [1.1566, 4.5017] \\ [2.1531, 4.7998] & [0.1415, 2.5154] \end{bmatrix}.$$

The quotient  $\eta$  can be used to translate these bounds into the bounds of the HIIA. In this case, it can be observed from the transfer function matrix in (8), that  $\gamma_1$  and  $\gamma_2$  are affecting the process as uncertain gains. Therefore, the quotient matrix is insensitive to uncertainty as mentioned in Section 2, and is given by

$$\eta = \begin{bmatrix} 1 & 0.9897 \\ 0.9906 & 1 \end{bmatrix}. \quad (9)$$

The bounds of the unnormalized PM can therefore be converted into bounds of the unnormalized HIIA through  $\eta$  without added uncertainty. The uncertainty intervals for the Hankel norm calculated with the different methods are

Table 2: Intervals for the sum of the elements for the decentralized pairings for the considered bounds in Case 1.

$[\cdot]$	$[\cdot]_{11} + [\cdot]_{22}$	$[\cdot]_{12} + [\cdot]_{21}$
$\tilde{\Sigma}_H^N$	[0.9609, 2.6629]	[2.5172, 4.2711]
$\tilde{\Phi}^N$	[0.4835, 3.6751]	[3.3097, 9.3057]

$$\Sigma_H^{(6)} \in \left[ \begin{array}{cc} [0.1192, 1.5233] & [0.1517, 2.9768] \\ [1.1031, 2.5072] & [-0.5489, 2.2762] \end{array} \right],$$

$$\tilde{\Sigma}_H^{(7)} \in \left[ \begin{array}{cc} [0.1192, 1.5233] & [0.1663, 2.9622] \\ [1.1097, 2.5006] & [-0.5489, 2.2762] \end{array} \right],$$

$$\tilde{\Sigma}_H^N \in \left[ \begin{array}{cc} [0.5848, 1.0769] & [1.0644, 2.0998] \\ [1.4536, 2.1703] & [0.3762, 1.5860] \end{array} \right].$$

$\Delta A$  is  $0_{4 \times 4}$ , and all  $\eta_{ij} \simeq 1$  which means that the difference between the bounds obtained from (6) and from (7) is small. For subsystem (4, 4),  $\Delta \tilde{\Sigma}_H^{(6)}$  and  $\Delta \tilde{\Sigma}_H^{(7)}$  overestimate the uncertainty since the lower bound is negative which is not realistic since the elements of  $\tilde{\Sigma}_H$  are always nonnegative. Negative elements should at this stage be replaced by 0 [9].

The Nyquist diagram approach gives a numerical approximation of the analytical bounds of the unnormalized HIIA and unnormalized PM. Clearly, the bounds derived from (7) largely overestimate the uncertainty since almost all of the lower bounds are negative.

Tab. 2 can be inspected to take robust decisions on control structure selection. There, intervals for the sum of the diagonal and the off-diagonal elements of the unnormalized HIIA and PM are given. Since these intervals overlap, the most suitable decentralized pairing varies between the different possible models in the uncertainty set. This makes it difficult to give a decentralized pairing recommendation. The uncertainty induced in the DNA can be graphically inspected in Fig. 2.

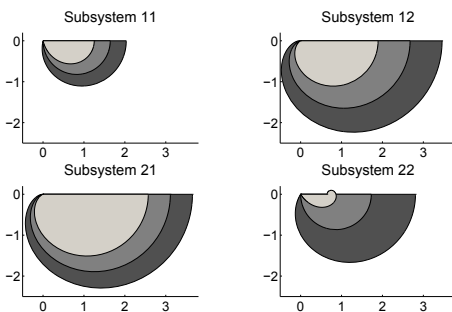


Figure 2: Nyquist diagrams with uncertainty regions for each subsystem in Case 1. The integration of the light grey area provides a lower bound for the PM, the light grey plus the grey areas provides the nominal value, and the total area including the dark grey area provides an upper bound.

Table 3: Intervals for the sum of the elements for the decentralized pairings for the considered bounds in Case 2. The last column indicates if the intervals overlap.

$[\cdot]$	$[\cdot]_{11} + [\cdot]_{22}$	$[\cdot]_{12} + [\cdot]_{21}$	Overlap
$\tilde{\Sigma}_H^{(6)}$	[0.0000, 4.4202]	[0.6074, 6.1314]	Yes
$\tilde{\Sigma}_H^{(7)}$	[0.7178, 2.6520]	[2.4028, 4.3359]	Yes
$\tilde{\Phi}^{(7)}$	[0.0000, 3.5302]	[1.9908, 9.6466]	Yes
$\tilde{\Phi}^{Sim}$	[1.2909, 1.5951]	[5.2789, 6.5372]	No

Case 2. A variation of  $[\Delta A]_{22} = 0.10[A]_{22} \neq 0$  for the quadruple-tank system in (4) is now considered. This corresponds to a 10% additive uncertainty in the parameter  $T_2$ . This results in a  $\Delta A$  matrix of rank 1, and therefore, this example renders the possibility to illustrate a comparison of the proposed tighter bounds given by (7) with the ones obtained from (6). The transfer function of the system in (8) reveals that the uncertainty in  $T_2$  only affects the second output.

Simulations reveal that the quotient matrix  $\eta$  only differs (by less than 0.1%) in one element (2,1) between the realizations of the uncertain system. Therefore, the nominal  $\eta$  in (9) is used in this example.

The uncertainty intervals for the Hankel norm obtained using (6) and (7), are then calculated to

$$\Sigma_H^{(6)} \in \left[ \begin{array}{cc} [-0.3720, 2.0145] & [0.3207, 2.8078] \\ [0.2867, 3.3235] & [-0.6784, 2.4057] \end{array} \right],$$

$$\tilde{\Sigma}_H^{(7)} \in \left[ \begin{array}{cc} [0.3993, 1.2431] & [1.1291, 1.9994] \\ [1.2737, 2.3366] & [0.3184, 1.4089] \end{array} \right].$$

The tightening of the bounds obtained with (7) significantly reduces the uncertainty intervals compared to the ones obtained from (6).

In order to obtain a quantification of the tightness of the bounds created with (7), a Monte Carlo simulation with 1000 realizations was performed. The worst case values of  $\tilde{\Phi}$  are then collected in  $\tilde{\Phi}^{Sim}$ , and compared with  $\tilde{\Phi}^{(7)}$ :

$$\tilde{\Phi}^{(7)} \in \left[ \begin{array}{cc} [-0.1965, 1.5453] & [0.9150, 4.0814] \\ [1.0758, 5.5652] & [-0.4931, 1.9849] \end{array} \right],$$

$$\tilde{\Phi}^{Sim} \in \left[ \begin{array}{cc} [0.6744, 0.6744] & [2.4980, 2.4980] \\ [2.7809, 4.0392] & [0.6165, 0.9207] \end{array} \right].$$

The bounds given by the inequalities are clearly too large, obtaining for both approaches negative values of the lower bounds for some of the elements in  $\tilde{\Phi}$  and  $\tilde{\Sigma}_H$ . Moreover, as pointed out earlier, only the second output of the system should be affected by the uncertainty in  $T_2$ . This is not reflected by the inequalities (7 and 6) since the same  $\Delta A$  is used for all subsystems. Obviously, this particular example reveals a weakness of this approach.

Inspecting Tab. 3, it is clear from  $\tilde{\Phi}^{Sim}$  that the preferred decentralized pairing should be the off-

diagonal. The same conclusion can be reached by inspecting Fig. 3. However, the large overestimation of the bounds derived from both inequalities (7 and 6), results in an overlap of the intervals in Tab. 3, which does not allow to take any robust decision on the decentralized pairing to be selected.

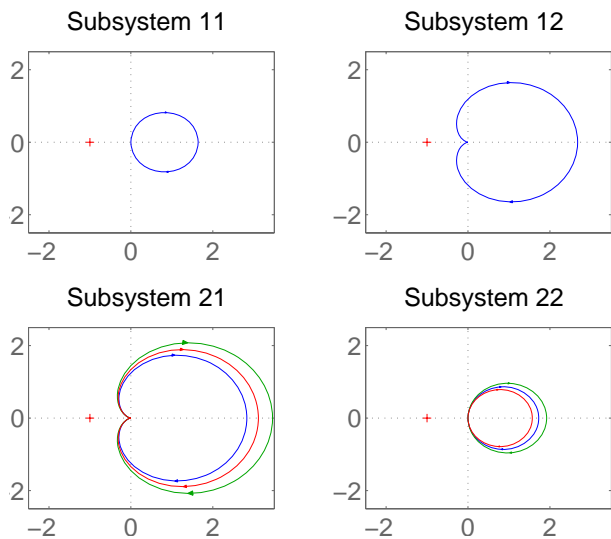


Figure 3: Nyquist diagrams for each subsystem in Case 2 with uncertainty bounds obtained from simulations.

## 5 Conclusions

In this paper, the uncertainty bounds for the HIIA of a system with additive parametric uncertainty derived in [9] were considered and further improved. The suggested modifications resulted in tighter bounds and allowed to derive uncertainty bounds for the PM. However, despite the improvement of the bounds, the affect of uncertainties is still overestimated to a degree that prevents the user from taking robust decisions on a feasible control structure. As an example, in many cases, negative lower bounds for the HIIA and PM were estimated, which is outside the possible value range of the IM:s.

A numerical approach of calculating the uncertainty bounds of the PM was suggested where the link between the PM and the Nyquist diagram was utilized. The approach is based on calculating the area enclosed by the Nyquist diagram for each subsystem with its corresponding uncertainty. The uncertainty bounds obtained this way resulted in non-negative values for HIIA and PM elements in the examples and was found to provide the tightest bounds. Furthermore, the Nyquist diagram provides a graphical interpretation of the PM, where the impact of additive uncertainties on the PM is represented by the area be-

tween the Nyquist curve for the nominal system and the Nyquist curve for the perturbed system.

Further research will focus on analytical solutions for the uncertainty bounds in order to provide users with robust interaction measures.

## References:

- [1] A. C. Antoulas. Frequency domain representation and singular value decomposition. UNESCO EOLSS (Encyclopedia for the Life Sciences), Contribution 6.43.13.4, June 2001.
- [2] E. H. Bristol. On a new measure of interaction for multivariable process control. *IEEE Trans. Automatic Control*, AC-11:133–134, 1966.
- [3] D. Chen and D. Seborg. Robust Nyquist array analysis based on uncertainty descriptions from system identification. *Automatica*, 38(3):467–475, 2002.
- [4] A. Conley and M. E. Salgado. Gramian based interaction measure. In *Proc. of the 39th IEEE Conf. on Decision and Control*, pages 5020–5022, Sydney, Australia, December 2000.
- [5] B. Hanzon. The area enclosed by the (oriented) nyquist diagram and the Hilbert-Schmidt-Hankel norm of a linear system. *IEEE Trans. on Automatic Control*, 37:835–839, 1992.
- [6] N. Jensen, D. G. Fisher, and S. L. Shah. Interaction analysis in multivariable control systems. *AIChE Journal*, 32(6):959–970, 1986.
- [7] K. H. Johansson. The quadruple-tank process: A multivariable laboratory process with an adjustable zero. *IEEE Trans. on Control Systems Technology*, 8(3):456–465, May 2000.
- [8] M. Kinnaert. Interaction measures and pairing of controlled and manipulated variables for multiple-input multiple-output systems: A survey. *Fuzzy Sets and Systems*, 36(4):15–23, 1995.
- [9] B. Moaveni and A. Khaki-Sedigh. Input-output pairing analysis for uncertain multivariable processes. *J. Process Control*, 18:527–532, 2008.
- [10] K. B. Petersen and M. S. Pedersen. The matrix cookbook. Technical University of Denmark, oct 2008.
- [11] M. E. Salgado and A. Conley. MIMO interaction measure and controller structure selection. *Int. J. Control*, 77(4):367–383, 2004.
- [12] S. Skogestad and I. Postlethwaite. *Multivariable Feedback Control*. John Wiley & Sons, Chichester, UK, 1996.
- [13] B. Wittenmark and M. E. Salgado. Hankel-norm based interaction measure for input-output pairing. In *Proc. of the 2002 IFAC World Congress*, Barcelona, Spain, 2002.